European Journal of Human Genetics (2017), 1–6
© 2017 Macmillan Publishers Limited, part of Springer Nature. All rights reserved 1018-4813/17
www.nature.com/ejhg

ARTICLE

Exome sequencing revealed a splice site variant in the *IQCE* gene underlying post-axial polydactyly type A restricted to lower limb

Muhammad Umair[1,2], Khadim Shah[1], Bader Alhaddad[2,3], Tobias B Haack[2,3], Elisabeth Graf[2,3], Tim M Strom[2,3], Thomas Meitinger[2] and Wasim Ahmad*[,1]

Polydactyly is characterized by an extra supernumerary digit/toe with or without bony element. To date variants in four genes *GLI3*, *ZNF141*, *MIPOL1* and *PITX1* have been implicated in developing non-syndromic form of polydactyly. The present study involved characterization of large consanguineous family of Pakistani origin segregating post-axial polydactyly type A, restricted to lower limb, in autosomal recessive pattern. DNA of two affected members in the family was subjected to exome sequencing. Sanger sequencing was then followed to validate segregation of the variants in the family members. A homozygous splice acceptor site variant (c.395-1G > A) was identified in the *IQCE* gene, which completely co-segregated with post-axial polydactyly phenotype within the family. The homozygous variant was absent in different public variant databases, 7000 in-house exomes, 130 exomes from unrelated Pakistani individuals and 215 ethnically matched controls. Mini-gene splicing assay was used to test effect of the variant on function of the gene. The assay revealed loss of first nucleotide of exon 6, producing a −1 frameshift and a premature stop codon 22 bases downstream of the variant (p.Gly132Valfs*22). The study provided the first evidence of involvement of the *IQCE* gene in limbs development in humans.
European Journal of Human Genetics advance online publication, 10 May 2017; doi:10.1038/ejhg.2017.83

INTRODUCTION

Polydactyly (Poly = many; dactylos = digits) is mainly characterized by supernumerary digits/toe, which is either fully developed with the bony element or an additive soft tissue without any bone element. Polydactyly is an inherited limb anomaly with an incidence between 5–19/10 000 live births and rudimentary skin tags are the most common ones.[1–3] Involvement of the lower limbs have been reported to be less common than the upper limbs, left hand less common than the right hand and the right foot is less common than the left foot.[4] It appears in combination with other phenotypes or a part of some developmental syndrome (syndromic polydactyly) or can appear as an isolated entity without any other malformation (non-syndromic).[5]

According to the most recent classification, non-syndromic polydactyly has been classified into post-axial polydactyly (PAP), axial (central) polydactyly and pre-axial polydactyly (PPD) according to the position of extra digit (s).[3,6] The PAP involves extra digit at fifth digit/toe and the least common type, axial (central) polydactyly characterized by duplication of central three digits (second, third or the fourth) and PPD involves a supernumerary digit/toe affecting the first digits/toe (thumb).[7,8] In addition, other complex types of polydactylies like palmar/ventral and dorsal type polydactyly, haas-type polysyndactyly and mirror image polydactyly (MIP) have been reported in the literature.[3,9]

The PAP is classified into two broad categories type A and B. It depends on either the development of an extra digit (PAP-type A) or not fully developed (rudimentary) classified as PAP-type B.[7] PAP-type A is further classified into six genetic types: PAP-type A1, PAP-type A2, PAP-type A3, PAP-type A4, PAP-type A5 and PAP-type A6.[6] In humans ten loci and four disease causing genes have been reported to cause different types of non-syndromic polydactylies. This includes a GLI family zinc finger 3 gene (*GLI3*, MIM 165240); a zinc finger protein 141 gene (*ZNF141*, MIM 194648); a mirror image polydactyly gene (*MIPOL1*, MIM 606850) and a paired like homeodomain 1 gene (*PITX1*, MIM 602149) (Table 1).

Previously, we have reported the first locus for autosomal recessive PAP-type A5 and a novel gene *ZNF141* in a family segregating PAP-type 6.[10,11] In the present study, we have presented another consanguineous family of Pakistani origin segregating PAP. Whole-exome sequencing (WES) identified a biallelic splice acceptor site variant (c.395-1G > A; p.Gly132Valfs*22) in the *IQCE* gene located on the chromosome 7p22.3.

MATERIALS AND METHODS

Study approval

The present study was performed following the declaration of Helsinki protocols, approved by the Institutional Review Board (IRB) of Quaid-i-Azam University, Islamabad, Pakistan and Institutional Review Board of Technical University Munich Germany. Written informed consent for conducting the study and for publication of radiographs and photographs were obtained from the family members.

[1]Department of Biochemistry, Faculty of Biological Sciences, Quaid-i-Azam University, Islamabad, Pakistan; [2]Institute of Human Genetics, Technische Universitat Munchen, Munchen, Germany; [3]Institute of Human Genetics, Helmholtz Zentrum Munchen, Neuherberg, Germany
*Correspondence: Professor W Ahmad, Department of Biochemistry, Faculty of Biological Sciences, Quaid-i-Azam University, Islamabad, Pakistan. Tel/Fax: +92 51 90643003; E-mail: wahmad@qau.edu.pk
Received 3 December 2016; revised 10 April 2017; accepted 13 April 2017

Table 1 Characterization of disease causing non-syndromic polydactyly types

Genes	*Disease*	*Inheritance*	*Locus*	*OMIM*
U	PPD1	AD	U	174400
ZRS/SHH	PPD2	AD	7q36	174500
U	PPD3	AD	U	174600
GLI3	PPD IV	AD	7p14.1	174700
U	HALLUX TYPE	U	2q31.1-31.2	601759
GLI3	PAPA1	AD	7p14.1	174200
U	PAPA2	AD	13q21-q32	602085
U	PAPA3	AD	19p13.1-p13.2	607324
U	PAPA4	AD	7q21-q34	608562
U	PAPA5	AR	13q13.3-q21.2	263450
ZNF141	PAPA6	AR	4p16.3	615226
MIPOL1	COMPLEX TYPE; MIP	AD	14.11.2-13	606850
PITX1	MIRROR IMAGE POLYDACTYLY	AD	5q31.1	602149
ZRS/SHH	HAAS TYPE	AD	7q36	186200

Abbreviations: AR, autosomal recessive; AD, autosomal dominant; U, unknown.

Isolation of genomic DNA

Peripheral blood samples were obtained from nine individuals including five unaffected (III-2, III-3, III-4, IV-3, IV-7) and four affected (IV-1, IV-2, IV-5, IV-6) in EDTA containing vacutainer sets (BD, Franklin Lakes, NJ, USA). Genomic DNA was extracted from whole blood using GenElute Blood Genomic DNA Kit (Sigma-Aldrich, St Louis, MO, USA). Extracted DNA was quantified using Nanodrop-1000 spectrophotometer (Thermal Scientific, Wilmington, St Louis, MA, USA).

Whole-exome sequencing

WES was performed using DNA extracted from blood of two affected members (Figure 1a). Enrichment of exomic sequences was carried out using SureSelect XT Human All Exon 50 Mb kit version 5 (Agilent Technologies, Santa Clara, CA, USA). Sequencing was performed on HiSeq 2500 systems (Illumina, San Diego, CA, USA) using Burrows-Wheeler Aligner (http://bio-bwa.sourceforge.net), and all reads were aligned against human assembly hg19 (GRCh37). SAM tools (http://samtools.sourceforge.net/) and PINDEL (http://gmt.genome.wustl.edu/packages/pindel/) were used for variant calling. Subsequently, filtering of the variants was performed with the help of the SAM tools varFilter and custom scripts. All the variants obtained after filtering were then inserted into an in-house database. Since the pedigree clearly depicts autosomal recessive inheritance of the phenotype (Figure 1a), therefore to discover putative pathogenic (affects function) homozygous recessive variants, we queried the database to show only those variants in both the affected individuals that were rare homozygous and disease causing.

Bioinformatics analysis

Frequency of the selected variants was further cross checked with in-house 7000 exomes, Exome Variant Server (http://evs.gs.washington.edu/EVS/), Exome Aggregation Consortium ExAC (http://exac.broadinstitute.org/), 1000 Genomes (http://www.1000 genomes.org) and dbSNP (http://www.ncbi.nlm.nih.gov/SNP/). Variants effect on the nearest splice site was predicted using NNSplice (Berkeley, CA, USA),[12] MutPred Splice (v1.3.2),[13] SKIPPY[14] and Human Splice Finder (v2.4.1).[15]

Sanger sequencing validation

The homozygous sequence variant, identified here, was verified by bidirectional Sanger sequencing in all members of the family. Primers were designed using Exon Primer (http://ihg.gsf.de).

Splicing assay

To study effect of the variant on splicing mechanism, we employed a mini-gene assay, which was based on a strategy originally developed for exon trapping.[16] A ~1900 bp fragment, containing *IQCE* exon 5–6 and ~350 bp of the neighboring introns, were PCR-amplified from genomic DNA of affected and normal individual using High Fidelity Phusion polymerase (Thermo Scientific, Pittsburgh, USA). As high fidelity Phusion polymerase produces blunt ended PCR product, therefore 0.7–1 unit of Taq DNA polymerase was added per tube, incubated at 72 °C for 10 min and placed on ice. Two distinct primers were designed (forward: 5′-AACAAAACCTCCCATTGTGTGTGCTTGT-3′ and reverse: 5′-TGGTTGTAACAAGTGGTTCTGCCCG-3′) and the resulting product was cloned into PCDNA (3.1a) TOPO vector using the TOPO TA Cloning according to manufacturer's protocol (Life Technologies, Carlsbad, CA, USA). Plasmids were analyzed by direct Sanger sequencing and then transfected into HeLa cells (105 cells in 3.5 cm wells). Total RNA was extracted using the Nucleospin RNA extraction kit (Macherey-Nagel Inc, Bethlehem, PA, USA), retrotranscribed with the Superscript III reverse transcriptase (Invitrogen, Carlsbad, CA, USA), and the resulting cDNA was PCR-amplified using primers designed from within exon 5 (forward: 5′AGTCTGACCCAGGCCCT3′) and exon 6 (reverse: 5′CTTCTTTAACTCAATAATCTCGTCA3′) of the *IQCE* gene. The amplified products were analyzed on 1.5% agarose gel electrophoresis and subsequently sequenced by dideoxy chain termination method. All the variants (Supplementary Table 4) have been submitted to the Leiden Open Variation Database (LOVD) at www.LOVD.nl/KREMEN1 (submission ID 00095221; Variant ID 0000154206).

RESULTS

Clinical description

Four affected members, in the family presented here, were diagnosed with PAP on the basis of the observed phenotypes and radiological examinations. Although, phenotypic variability was observed among affected individuals (IV-1, IV-2, IV-5, IV-6), but the condition was found restricted only to feet. An affected individual (IV-5) showed brachymetatarsia of 5th toe in the right foot (Figure 1c), and affected individual (IV-6) had PAP only in the right foot (Figure 1d).

Radiological examination of affected individuals (IV-1, IV-2) showed radial varus deviation of 4th and 5th toes in both feet, and varus deviation of 5th toe of right foot in affected individual (IV-5). Bilateral syndactyly of 2nd and 3rd toe was observed only in an affected individual (IV-1). All the affected individuals had well developed nails in the extra toes. Radiographical analysis revealed that both 5th and 6th toes (digits) in the affected individuals were attached to the two headed thick broad 5th metatarsal (Figures 1b–d). The 5th metatarsal in the right foot in affected individual (IV-5) had valgus deviation, while both 5th and 6th toes had cubitus varus deviation as well.

All the affected individuals had normal height and weight. Abnormalities involving heart, kidney, nails, teeth, hearing, and brain were not observed in any affected member. Heterozygous carrier individuals had no abnormality, and were phenotypically and clinically indistinguishable from other normal individuals.

WES and sanger sequencing

To search for disease causing variants, WES was performed at Institute of Human Genetics, Helmholtz Zentrum, Munchen, Germany as described previously.[17] Variants screening was performed on the basis of autosomal recessive pattern of inheritance of the polydactyly phenotype, rare variants and OMIM list of syndromic and non-syndromic polydactyly genes presented in Supplementary Table 1. We focused only on pathogenic (affects function), disease causing non-synonymous (NS) variants, causing splice acceptor and donor site variants (SS), nonsense, missense, short frameshift coding deletions (indel) or insertions and large deletions/duplications. Total 82

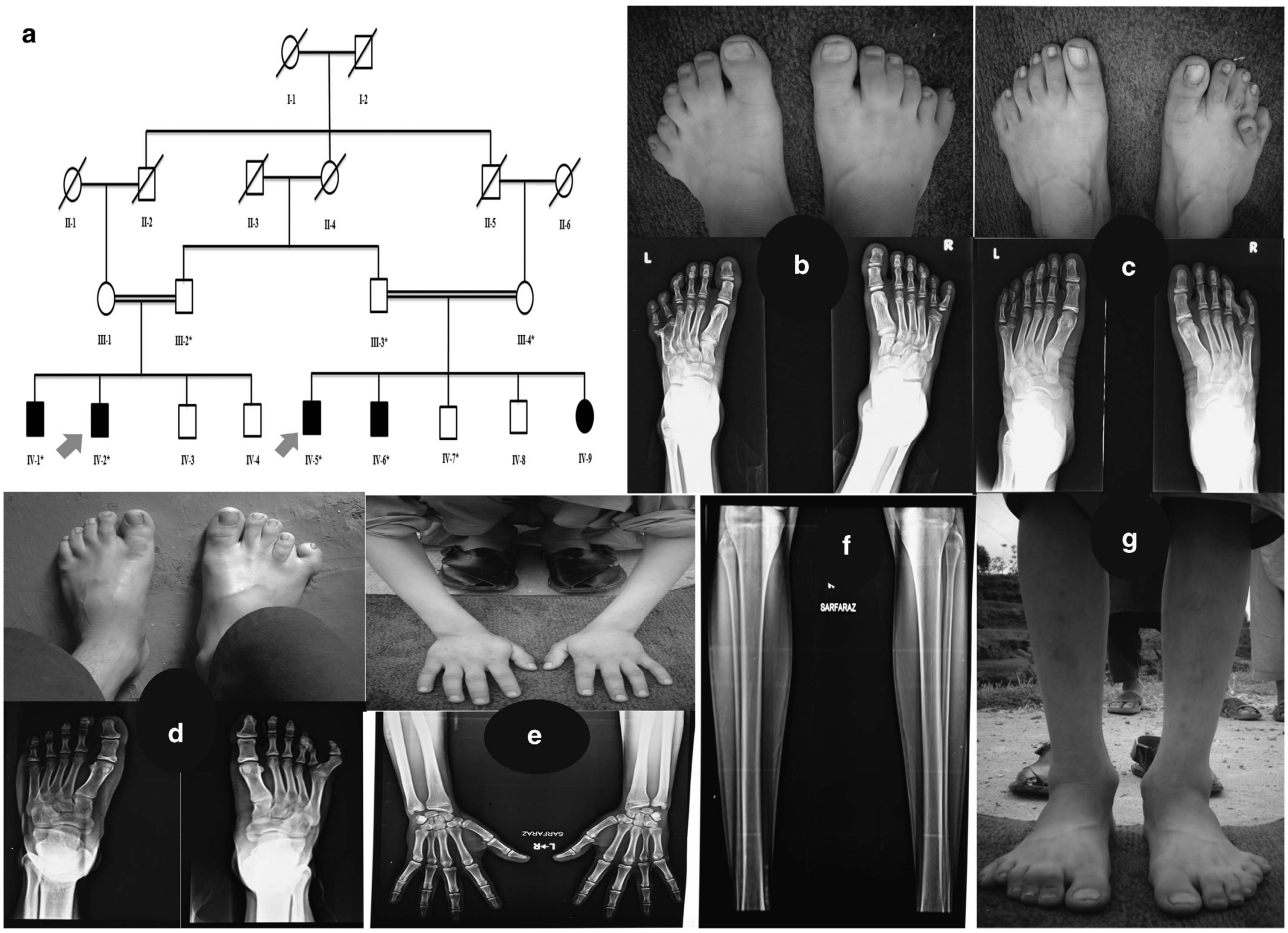


Figure 1 (**a**) Pedigree depicting autosomal recessive inheritance pattern of PAP. Clear circles and squares represent normal females and males, respectively. Filled symbols representing affected members. Double lines indicate consanguineous unions. Individual numbers labeled with asterisks indicate those who were available for the present study. Red arrows indicating affected individuals subjected to WES. (**b**) Image and radiographs of an affected individual IV-1 having bilateral PAP and incomplete syndactyly of 2nd and 3rd toe. Radiographs showing radial varus deviation of 4th and 5th toes in both feet, extra toes originating form 5th metatarsal. (**c**) Image and radiographs of affected individual (IV-5) having bilateral PAP with brachymetatarsia of 5th toe in the right foot. (**d**) Image and radiographs of an affected individual IV-6 showing unilateral PAP in the right foot. Radiographic analysis revealed varus deviation of the 5th and radial valgus deviation of the 6th toe with extra toe attached to the 5th metatarsal. (**e**) Image and radiographs of both hands of an affected individual IV-1 showing absence of polydactyly phenotype. (**f**) Lower limbs radiographs of IV-1 having normal tibia and fibula. (**g**) Lower limbs of IV-1 having normal length and normal tibia/fibula. All the affected individuals showed complete well developed nails in the extra toes. The full colour version of this figure is available at *European Journal of Human Genetics* online.

compound heterozygous or homozygous variants were detected in DNA of at least one of the affected individual subjected for exome sequencing (Supplementary Table 2). Exome statistics are presented in Supplementary Table 3. Considering polydactyly is a rare disorder and it is highly unlikely that the disease causing variant could be present in the general population therefore the data was cross-matched with online public databases.

Following step-by-step filtering process for screening homozygous and compound heterozygous variants, six homozygous variants were identified/filtered in six different genes including *MAD1L1* (MIM 602686), *IQCE, TNRC18, PNPLA4, LANCL2* and *BAG3* (MIM 603883). A splice acceptor site variant c.395-1G>A (NM_152558.4; NC_000007.14), in intron 5 of the *IQCE* gene, located on chromosome 7p22.3, was found to segregate with the disease phenotype as verified by Sanger sequencing (Supplementary Figure). The variant (c.395-1G>A) was not found in homozygous state in dbSNP, 1000 Genomes, EVS, internal database and ExAC and predicted to be deleterious in online available bioinformatics tools (Supplementary Table 4). In the ExAc database containing more than 60 000 human exome data, the *IQCE* variant (c.395-1G>A) was found three times in heterozygous state only with allele frequency of 0.0001818 in south Asian population. The variant is highly conserved across multiple species (Figure 2).To exclude polymorphic nature of the variant, it was cross checked within different online variant databases, 7000 in-house exome (IHG, Helmholtz, Munich, Germany), 130 exomes from unrelated Pakistani individuals, and 215 ethnically matched controls. *In silico* analyses clearly validated that the splice site variant has a strong impact on the normal splicing pattern of the gene, as expected for DNA changes involving -1 and -2 bases of intron acceptor sequences.

HeLa cells transfection using mini-gene constructs bearing this change and its wild-type counterpart revealed that (c.395-1G>A) affects the canonical splicing of exon 6 by knocking down its natural 3′ acceptor splice site and eliciting the use of a cryptic splice site, just one

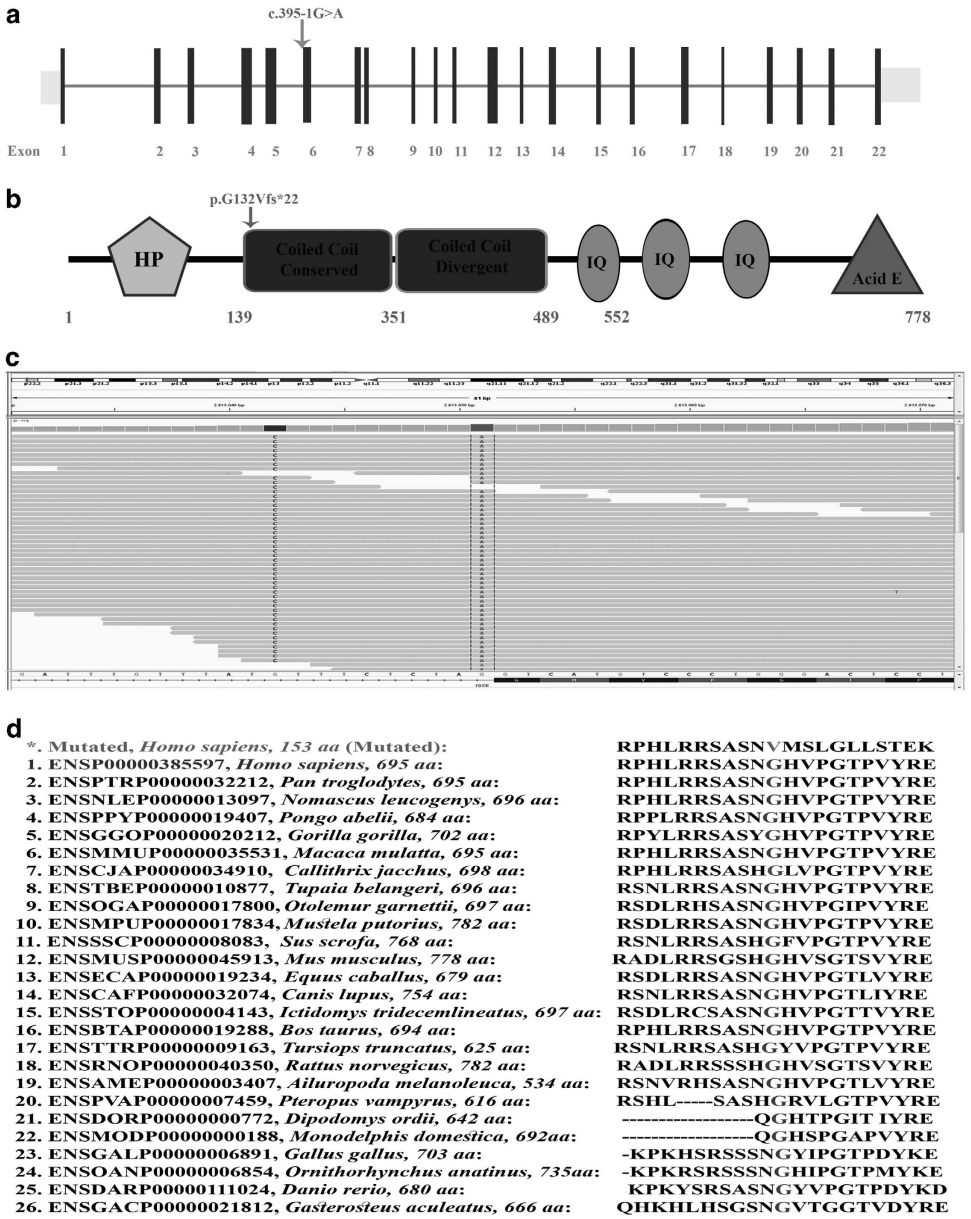


Figure 2 (**a**) *IQCE* gene structure showing the identified variant (red arrow). (**b**) The structure of the gene product (IQCE protein cartoon diagram) showing different domains and location of variant is represented with red arrow. (**c**) Visualization of WES data under the expert Integrative Genomics Viewer (IGV). The forward strand displaying the novel splice acceptor site variant in intron 5 of *IQCE* is shown in the affected individual. (**d**) Conservation of Glycine (G) residue across different species, which is changed into Valine (V) due to first G nucleotide deletion in exon 6 as a result of splice acceptor site variant (c.395-1G>A). Intronic regions are not drawn up to scale. The full colour version of this figure is available at *European Journal of Human Genetics* online.

base pair downstream of intron 3′s acceptor sequence (Figures 3a and b). This event led to the loss of first nucleotide of exon 6, producing a −1 frameshift and a premature stop codon 22 bases downstream of the variant (p.Gly132Valfs*22). We were unable to perform protein quantification due to refusal by the affected members to provide additional blood samples and skin biopsies.

DISCUSSION

In the present study, we have characterized a large consanguineous family segregating post-axial polydactyly type A (PAP-type A) in autosomal recessive manner. PAP phenotypes observed in affected members of the family were similar to those reported previously in families inheriting PAP-type A[11,18–20]. However, polydactyly restricted to feet only were not reported in these cases. Cutaneous syndactyly, involving 2nd and 3rd toes, was observed only in one affected member (IV-1) of the present family. This feature of cutaneous syndactyly, associated with PAP-type A/B in hands/feet, was reported previously by Galjaard *et al.*[19] Hallux valgus deformity, reported previously by Kalsoom *et al.*[11] was also observed in an affected member of the present family. Fork shaped metatarsal of the 5th toe, reported by Kalsoom *et al.*,[11] was missing in affected members of the present study. Instead the 5th and 6th toe were attached to the two headed broad 5th metatarsal. A condition called brachymetatarsia of 5th toe, observed in an affected individual (IV-6) in the present study, was not reported earlier.

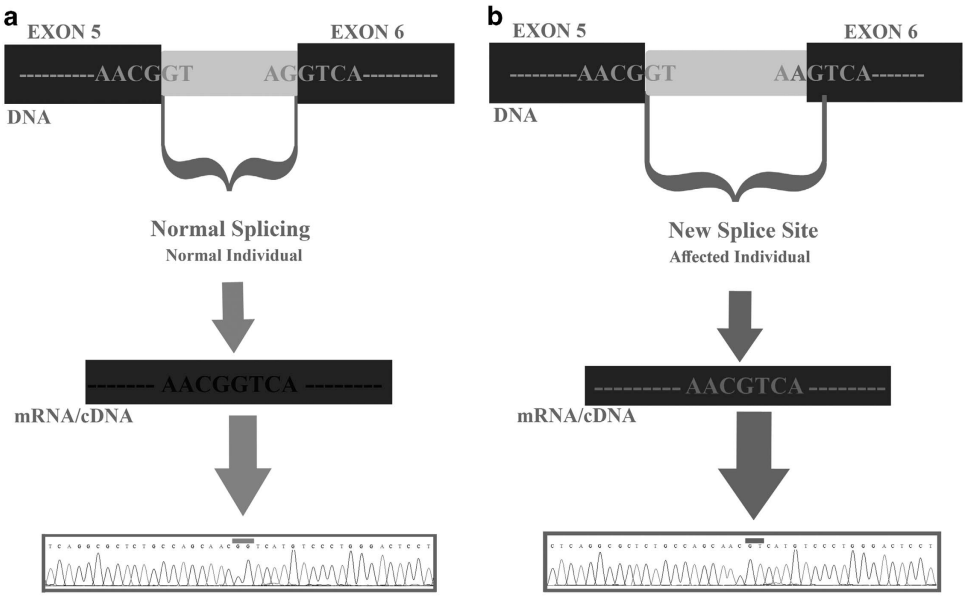


Figure 3 (**a**) Schematic demonstration of the effect of the splice acceptor site variant (c.395-1G>A) on IQCE mRNA using mini-gene assay technique. cDNA sequence showing construct from control DNA. (**b**) cDNA sequence showing DNA constructs bearing the variant.

Exome sequencing revealed a homozygous novel splice acceptor site variant (c.395-1G>A; NM_152558.4), segregating with the disease phenotype, in the family reported here. The variant was present in intron 5 of the *IQCE* gene mapped on chromosome 7p22.3. *In silico* analysis, verified by *in vitro* mini-gene assay, revealed the variant (c.395-1G>A) altered the splicing pattern of the *IQCE* gene, induced use of cryptic splice site and finally produced a frameshift leading to a premature termination codon (p.Gly132Valfs*22). However, since the mini-gene assay only included exons 5 and 6, therefore this cannot be validated that this is the only splicing alteration produced by the variant in patient cells. The variant, is predicted to result in truncated IQCE protein lacking the coiled coil conserved/diverged regions, three tandem α-helical IQ motifs involved in interaction of IQCE with EFCAB7, and C-terminal Acid E domain, affecting protein interactions and most likely degraded by nonsense mediated mRNA decay (NMD).[21]

In the *Iqce* knockout mouse (MGI:1921489), various types of skeletal deformities including pre-axial polydactyly (1/10 mice showed pre-axial polydactyly only in one lower limb), digit abnormalities, and short and long tibia were reported only in the lower limbs (http://www.mousephenotype.org/data/imageComparator?&parameter_stable_id=IMPC_XRY_034_001&acc=MGI:1921489). Additional features observed in *Iqce* knockout mouse including metabolism, behavior, skeleton, immune system, eyes and cardiovascular system abnormalities, that were missing in our family.[22,23] In the knockout mice, the gene *Iqce* was completely removed leading to different phenotypes than those reported in human here. In addition, several other factors including variable expressivity, incomplete penetrance, difference in genetic background, environmental influence and epigenetic phenomena probably played roles in developing differential phenotypes in human. Presence of long/short tibia phenotype in the knockout mice supported the notion that *Iqce* pathogenesis causes defects in lower limbs, thus supporting the data presented here.

EVC and EVC2 form a protein complex which has been identified as a tissue specific regulator of Hh signaling.[24–26] EVC and EVC2 bind to SMO and localize to EVC zone at the base of primary cilia, which is critical for Hh signaling. The IQCE-EFCAB7 module acts tethering the EVC–EVC2 complex (the EvC complex) to the base of the primary cilium.[21] EFCAB7 and IQCE both co-localize with EVC2 at the base of cilia in the EVC zone. Biochemical interactions and subcellular localization of IQCE and EFCAB7 suggested that they have important role in EVC–EVC2 complex regulation and regulating Hh signaling transduction.[21,27]

Dorn *et al.*[28] suggested that EVC–EVC2 complex is involved in regulation of SMO-GLI step in Hh signaling. Pusapati *et al.*[21] verified experimentally that IQCE-EFCAB7 complex play an important role in the step between SMO-GLI proteins and depletion of both IQCE and EFCAB7 affect the signaling by SMO and in turn affect Hh signaling.

In conclusion, we have used WES to identify the first sequence variant in the *IQCE* gene resulting in a non-syndromic form of PAP. This provided the first evidence in human that missing IQCE lead to abnormal limb development.

CONFLICT OF INTEREST

The authors declare no conflict of interest.

ACKNOWLEDGEMENTS

We highly appreciate cooperation and participation of the family members in this study. Muhammad Umair and Khadim Shah were supported by International Research Support Initiative Program (IRSIP) and Indigenous PhD fellowship (HEC) and from Higher Education Commission (HEC), Islamabad, Pakistan. This work was funded by Pakistan Academy of Science (PAS) Islamabad, Pakistan to Wasim Ahamad.

1 Schwabe GC, Mundlos S: Genetics of congenital hand anomalies. *Handchir Mikrochir Plast Chir* 2004; **36**: 85–97.
2 Christensen JC, Leff FB, Lepow GM *et al*: Congenital polydactyly and polymetatarsalia: classification, genetics, and surgical correction. *J Foot Ankle Surg* 2011; **50**: 336–339.
3 Malik S: Polydactyly: phenotypes, genetics and classification. *Clin Genet* 2014; **85**: 203–212.
4 Malik S, Ullah S, Afzal M, Lal K, Haque S: Clinical and descriptive genetic study of polydactyly: a Pakistani experience of 313 cases. *Clin Genet* 2014; **85**: 482–486.

5 Biesecker LG: Polydactyly: how many disorders and how many genes? 2010 update. *Develop Dyn* 2011; **240**: 931–942.
6 Deng H, Tan T, Yuan L: Advances in the molecular genetics of non-syndromic polydactyly. *Expert Rev Mol Med* 2015; **17**: 1–10.
7 Talamillo A, Bastida MF, Fernandez-Teran M, Ros MA: The developing limb and the control of the number of digits. *Clin Genet* 2005; **67**: 143–153.
8 Haber LL, Adams HB, Thompson GH, Duncan LS, Didomenico LA, McCluskey WP: Unique case of polydactyly and a new classification system. *J Pediatr Orthop* 2007; **27**: 326–328.
9 Phadke SR, Sankar VH: Polydactyly and genes. *Indian J Pediatr* 2010; **77**: 277–281.
10 Umm-e-Kalsoom, Basit S, Kamran-ul-Hassan Naqvi S, Ansar M, Ahmad W: Genetic mapping of an autosomal recessive postaxial polydactyly type A to chromosome 13q13.3-q21.2 and screening of the candidate genes. *Hum Genet* 2012; **131**: 415–422.
11 Kalsoom UE, Klopocki E, Wasif N *et al*: Whole exome sequencing identified a novel zinc-finger gene ZNF141 associated with autosomal recessive postaxial polydactyly type A. *J Med Genet* 2012; **50**: 47–53.
12 Reese MG, Eeckman FH, Kulp D, Haussler D: Improved splice site detection in Genie. *J Comput Biol* 1997; **4**: 311–323.
13 Mort M, Sterne-Weiler T, Li B *et al*: MutPred Splice: machine learning-based prediction of exonic variants that disrupt splicing. *Genome Biol* 2014; **15**: R19.
14 Woolfe A, Mullikin JC, Elnitski L: Genomic features defining exonic variants that modulate splicing. *Genome Biol* 2010; **11**: R20.
15 Desmet FO, Hamroun D, Lalande M, Collod-Béroud G, Claustres M, Béroud C: Human Splicing Finder: an online bioinformatics tool to predict splicing signals. *Nucleic Acids Res* 2009; **37**: e67.
16 Buckler AJ, Chang DD, Graw SL: Exon amplification: a strategy to isolate mammalian genes based on RNA splicing. *Proc Natl Acad Sci USA* 1991; **88**: 4005–4009.
17 Haack TB, Danhauser K, Haberberger B *et al*: Exome sequencing identifies ACAD9 mutations as a cause of complex I deficiency. *Nat Genet* 2010; **42**: 1131e4.
18 Zhao H, Tian Y, Breedveld G *et al*: Postaxial polydactyly type A/B (PAP-A/B) is linked to chromosome 19p13.1-13.2 in a Chinese kindred. *Eur J Hum Genet* 2002; **10**: 162–166.
19 Galjaard RJ, van der Linde HC, Eussen BH *et al*: Isolated postaxial polydactyly type B with mosaicism of a submicroscopic unbalanced translocation leading to an extended phenotype in offspring. *Am J Med Genet A* 2003; **121A**: 168–173.
20 Al-Qattan MM: A novel frameshift mutation of the GLI3 gene in a family with broad thumbs with/without big toes, postaxial polydactyly and variable syndactyly of the hands/feet. *Clin Genet* 2012; **82**: 502–504.
21 Pusapati GV, Hughes CE, Dorn KV *et al*: EFCAB7 and IQCE regulate hedgehog signaling by tethering the EVC-EVC2 complex to the base of primary cilia. *Dev Cell* 2014; **28**: 483–496.
22 Hansen GM, Markesich DC, Burnett MB *et al*: Large-scale gene trapping in C57BL/6 N mouse embryonic stem cells. *Genome Res* 2008; **18**: 1670–1679.
23 Eppig JT, Blake JA, Bult CJ, Kadin JA, Richardson JE: The Mouse Genome Database Group. 2015. The Mouse Genome Database (MGD): facilitating mouse as a model for human biology and disease. *Nucleic Acids Res* 2015; **28**: 43.
24 Blair HJ, Tompson S, Liu YN *et al*: Evc2 is a positive modulator of Hedgehog signalling that interacts with Evc at the cilia membrane and is also found in the nucleus. *BMC Biol* 2011; **9**: 14.
25 Ruiz-Perez VL, Blair HJ, Rodriguez-Andres ME *et al*: Evc is a positive mediator of Ihh-regulated bone growth that localises at the base of chondrocyte cilia. *Development* 2007; **134**: 2903–2912.
26 Caparrós-Martín JA, Valencia M, Reytor E *et al*: The ciliary Evc/Evc2 complex interacts with Smo and controls Hedgehog pathway activity in chondrocytes by regulating Sufu/Gli3 dissociation and Gli3 trafficking in primary cilia. *Hum Mol Genet* 2013; **22**: 124–139.
27 Lopez-Rios J: The many lives of SHH in limb development and evolution. *Semin Cell Dev Biol* 2016; **49**: 16–24.
28 Dorn KV, Hughes CE, Rohatgi R: A Smoothened-Evc2 complex transduces the Hedgehog signal at primary cilia. *Dev Cell* 2012; **23**: 823–835.

Supplementary Information accompanies this paper on European Journal of Human Genetics website (http://www.nature.com/ejhg)